J|A|C|S
ARTICLES
Published on Web 05/28/2004

Substituent Effects in $\pi-\pi$ Interactions: Sandwich and T-Shaped Configurations

Mutasem Omar Sinnokrot and C. David Sherrill*

Contribution from the Center for Computational Molecular Science and Technology, School of Chemistry and Biochemistry, Georgia Institute of Technology, Atlanta, Georgia 30332-0400

Received January 31, 2004; E-mail: sherrill@chemistry.gatech.edu

Abstract: Sandwich and T-shaped configurations of benzene dimer, benzene−phenol, benzene−toluene, benzene−fluorobenzene, and benzene−benzonitrile are studied by coupled-cluster theory to elucidate how substituents tune $\pi-\pi$ interactions. All substituted sandwich dimers bind more strongly than benzene dimer, whereas the T-shaped configurations bind more or less favorably depending on the substituent. Symmetry-adapted perturbation theory (SAPT) indicates that electrostatic, dispersion, induction, and exchange-repulsion contributions are all significant to the overall binding energies, and all but induction are important in determining relative energies. Models of π-π interactions based solely on electrostatics, such as the Hunter-Sanders rules, do not seem capable of explaining the energetic ordering of the dimers considered.

Introduction

Noncovalent interactions are of pivotal importance in many areas of chemistry, biology, and materials science,[1−3] and $\pi-\pi$ interactions in particular are fundamental to many supramolecular organization and recognition processes.[4] These interactions play a key role in phenomena as diverse as base−base interactions of DNA,[5] side-chain interactions in proteins,[6] host−guest complexation,[7] self-assembly based on synthetic molecules,[8,9] and intercalation of certain drugs into DNA.[10] Despite a wide body of theoretical and experimental studies addressing the importance of $\pi-\pi$ interactions,[11−21] a clear picture of their strength and geometrical preferences presents a challenge for both experiment and theory due to the weakness of the interactions and the shallowness of the potential energy surfaces. However, advances in rational supramolecular design will require a detailed understanding of these interactions and how substituent effects may tune them.

In previous work,[17] we provided the first definitive study of the simplest prototype of aromatic $\pi-\pi$ interactions, the benzene dimer. Using explicitly correlated MP2−R12/A[22] wave functions, we estimated the complete basis set limit gas-phase binding energies at the second-order Møller−Plesset perturbation theory (MP2) level. After accounting for higher-order electron correlation via coupled-cluster with singles, doubles, and perturbative triples [CCSD(T)],[23] the resulting binding energies should be within a few tenths of one kcal mol^{-1} of the ab initio limit. The estimated complete basis set CCSD(T) values of D_e (D_0) predict[17] that the T-shaped and parallel-displaced configurations are nearly isoenergetic, with binding energies of 2.7 (2.4) and 2.8 (2.7) kcal mol^{-1}, respectively. The face-to-face sandwich configuration is about 1 kcal mol^{-1} less stable. These results show that the commonly cited experimental binding energy of Krause et al. ($D_0 = 1.6 \pm 0.2$ kcal mol^{-1}) is too low by about one kcal mol^{-1}. That interacting pairs of phenylalanines in proteins are generally found in orientations similar to the T-shaped or parallel-displaced configurations[24,25] is consistent with our theoretical predictions that these two configurations are nearly isoenergetic.

Substituents, however, may alter the energy landscape. For toluene dimer in both aqueous solution and the gas phase, two stacked configurations are predicted to be more stable than the T-shaped configuration.[26] Very little is known about substituent effects in $\pi-\pi$ interactions, either theoretically or experimentally. A few studies have used NMR techniques to examine $\pi-\pi$

(1) Mulliken, R. S. *J. Am. Chem. Soc.* **1952**, *74*, 811.
(2) Hunter, C. A.; Sanders, J. K. M. *J. Am. Chem. Soc.* **1990**, *112*, 5525.
(3) Kumph, R. A.; Dougherty, D. A. *Science* **1993**, *261*, 1708.
(4) Meyer, E. A.; Castellano, R. K.; Diederich, F. *Angew. Chem., Int. Ed. Engl.* **2003**, *42*, 1210.
(5) Saenger, W. *Principles of Nucleic Acid Structure*; Springer-Verlag: New York, 1984.
(6) Burley, S. K.; Petsko, G. A. *Science* **1985**, *229*, 23.
(7) Hunter, C. A. *Chem. Soc. Rev.* **1994**, *23*, 101.
(8) Claessens, C. G.; Stoddart, J. F. *J. Phys. Org. Chem.* **1997**, *10*, 254.
(9) Glaser, R.; Dendi, L. R.; Knotts, N.; Barnes, C. L. *Cryst. Growth Des.* **2003**, *3*, 291.
(10) Lerman, L. S. *J. Mol. Biol.* **1961**, *3*, 18.
(11) Tsuzuki, T.; Uchimaru, T.; Tanabe, K. *J. Mol. Struct. (THEOCHEM)* **1994**, *307*, 107.
(12) Hobza, P.; Selzle, H. L.; Schlag, E. W. *J. Phys. Chem.* **1996**, *100*, 18 790.
(13) Tsuzuki, S.; Lüthi, H. P. *J. Chem. Phys.* **2001**, *114*, 3949.
(14) Steed, J. M.; Dixon, T. A.; Klemperer, W. *J. Chem. Phys.* **1979**, *70*, 4940.
(15) Arunan, E.; Gutowsky, H. S. *J. Chem. Phys.* **1993**, *98*, 4294.
(16) Law, K. S.; Schauer, M.; Bernstein, E. R. *J. Chem. Phys.* **1984**, *81*, 4871.
(17) Sinnokrot, M. O.; Valeev, E. F.; Sherrill, C. D. *J. Am. Chem. Soc.* **2002**, *124*, 10 887.
(18) Felker, P. M.; Maxton, P. M.; Schaeffer, M. W. *Chem. Rev.* **1994**, *94*, 1787.
(19) Venturo, V. A.; Felker, P. M. *J. Chem. Phys.* **1993**, *99*, 748.
(20) Tsuzuki, S.; Honda, K.; Uchimaru, T.; Mikami, M.; Tanabe, K. *J. Am. Chem. Soc.* **2002**, *124*, 104.
(21) Hobza, P.; Jurečka, P. *J. Am. Chem. Soc.* **2003**, *125*, 15 608.
(22) Kutzelnigg, W.; Klopper, W. *J. Chem. Phys.* **1991**, *94*, 1985.
(23) Raghavachari, K.; Trucks, G. W.; Pople, J. A.; Head-Gordon, M. *Chem. Phys. Lett.* **1989**, *157*, 479.
(24) Hunter, C. A.; Singh, J.; Thornton, J. M. *J. Mol. Biol.* **1991**, *218*, 837.
(25) McGaughey, G. B.; Gagné, M.; Rappé, A. K. *J. Biol. Chem.* **1998**, *273*, 15 458.
(26) Chipot, C.; Jaffe, R.; Maigret, B.; Pearlman, D. A.; Kollman, P. A. *J. Am. Chem. Soc.* **1996**, *118*, 11 217.

10.1021/ja049434a CCC: $27.50

Chart 1

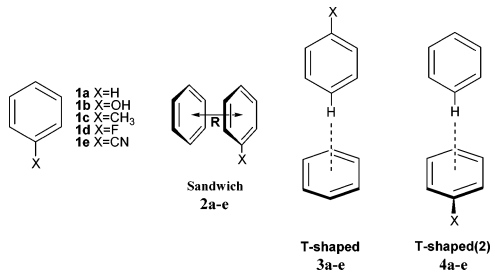

interactions in substituted aromatics. Cozzi, Siegel, and co-workers[27−29] have measured barrier heights to rotation in substituted 1,8-diarylnaphthalenes featuring a face-to-face (sandwich) arrangement. Rashkin and Waters recently reported experiments on substituent effects in a model system with an offset-stacked (parallel-displaced) configuration.[30] Wilcox and co-workers devised a "molecular torsion balance" model system to examine substituent effects on perpendicular (T-shaped) $\pi-\pi$ interactions.[31,32] Hunter and co-workers have also examined T-shaped configurations using chemical double-mutant cycles and molecular zipper complexes.[33,34] Because none of these experiments were performed in the gas phase, it is difficult to decouple the intrinsic binding energy from contributions due to the solvent or environment, which will change from system to system.[35] Additionally, due to secondary intramolecular interactions or steric constraints, the model system itself may complicate the interpretation of results.[36] Although theory can examine the bare interactions directly, experience with the benzene dimer[17] indicates that this is challenging, because coupled-cluster theory and augmented triple-ζ or better basis sets are required for reliable total binding energies. Systematic theoretical studies of substituent effects in $\pi-\pi$ interactions seem to be entirely absent, apart from a double-ζ MP2 study of T-shaped configurations by Hong and Kim.[37]

In a recently published letter,[38] we presented preliminary results from the first ab initio study of substituent effects in face-to-face (sandwich) $\pi-\pi$ interactions. Dimers of benzene with monosubstituted benzenes were considered, with substituents OH, CH_3, F, and CN (**2** in Chart 1). The most surprising result was that *all* substituted dimers bind more strongly than benzene dimer, regardless whether the substituents are considered electron donating (OH, CH_3) or electron withdrawing (CN, F), in apparent contradiction to the Hunter-Sanders model.[2] While acknowledging that dispersion has a major effect on the magnitude of $\pi-\pi$ interactions, the Hunter−Sanders model makes qualitative predictions assuming that geometries and substituent effects are determined by electrostatic interactions, with the π electron clouds being negatively charged and the σ framework being positively charged. Other effects, such as induction and short-range repulsion, are ignored. According to this model, electron-donating groups such as OH should increase the negative charge of the electron clouds on the substituted monomer, leading to increased repulsion in the sandwich dimer. This expectation does not fit our high-level theoretical results. A preliminary analysis of our data for the sandwich dimers suggested that it is not possible to understand the trends in binding based on electrostatic effects alone.[38]

In this work, we explore how substituents affect the binding of the T-shaped configuration (**3** and **4**). When substituting the upper ring in the T-shaped configuration (**3**), the substituent is placed only in the position para to the other benzene to minimize complications from direct interactions between the substituent and the other benzene. Likewise, when the lower ring is substituted (**4**), the substituent is placed as far away from the edges of the upper benzene as possible. We also extend our preliminary report on the sandwich dimers (**2**) by incorporating CCSD(T) corrections into the geometry optimization. This has a nonnegligible effect on the total binding energies. Using an additive correction scheme, we estimate interfragment distances and binding energies at the highly reliable CCSD(T)/aug-cc-pVTZ level of theory. Lower levels of theory are also considered to investigate which ones are capable of accurately reproducing changes in binding due to substituents. Surprisingly, even though total binding energies are very sensitive to basis set and electron correlation, the relative energies for different substituted dimers are not. To further investigate the relative importance of electrostatic, dispersion, induction, and exchange-repulsion energies we have decomposed binding energies into these components using symmetry-adapted perturbation theory (SAPT).[39,40] This analysis confirms that electrostatic interactions alone are not sufficient to predict the correct energetic ordering of all the dimers.

Theoretical Methods

Supermolecular Approach. Most computations were performed using Dunning's augmented correlation-consistent polarized valence basis sets,[41] specifically the double- and triple-ζ basis sets aug-cc-pVDZ and aug-cc-pVTZ. The aug- prefix denotes the presence of one set of diffuse functions for each angular momentum in the basis; this adds a considerable number of diffuse functions to the standard, unaugmented cc-pVXZ basis sets. In a previous study of benzene dimer,[17] we found that augmenting the cc-pVDZ basis with diffuse functions was more important to the binding energy than increasing the basis set to cc-pVTZ. In that study we also explored basis set convergence by using basis sets as large as quadruple-ζ aug-cc-pVQZ (1512 basis functions), and complete basis set estimates were obtained using the explicitly correlated MP2−R12/A method.[22] Unfortunately, such sophisticated computations are not yet feasible for all of the lower-symmetry substituted dimers in the present study due to their prohibitively high computational cost. Our previous benchmark results are reproduced here for comparison to the levels of theory presently employed.

Monomers were fully optimized at the MP2/aug-cc-pVDZ and MP2/aug-cc-pVTZ levels of theory. For toluene, there is almost free rotation of the methyl group, so we chose a one H up, 2 H down, C_s configuration. Dimer geometries were determined by optimizing the

(27) Cozzi, F.; Ponzini, F.; Annunziata, R.; Cinquini, M.; Siegel, J. S. *Angew. Chem., Int. Ed. Engl.* **1995**, *34*, 1019.
(28) Cozzi, F.; Siegel, J. S. *Pure Appl. Chem.* **1995**, *67*, 683.
(29) Cozzi, F.; Cinquini, M.; Annunziata, R.; Dwyer, T.; Siegel, J. S. *J. Am. Chem. Soc.* **1992**, *114*, 5729.
(30) Rashkin, M. J.; Waters, M. L. *J. Am. Chem. Soc.* **2002**, *124*, 1860.
(31) Paliwal, S.; Geib, S.; Wilcox, C. S. *J. Am. Chem. Soc.* **1994**, *116*, 4497.
(32) Kim, E.; Paliwal, S.; Wilcox, C. S. *J. Am. Chem. Soc.* **1998**, *120*, 11 192.
(33) Adams, H.; Carver, F. J.; Hunter, C. A.; Morales, J. C.; Seward, E. M. *Angew. Chem., Int. Ed. Engl.* **1996**, *35*, 1542.
(34) Carver, F. J.; Hunter, C. A.; Livingstone, D. J.; McCabe, J. F.; Seward, E. M. *Chem. Eur. J.* **2002**, *8*, 2848.
(35) Nakamura, K.; Houk, K. N. *Org. Lett.* **1999**, *1*, 2049.
(36) Ribas, J.; Cubero, E.; Luque, F. J.; Orozco, M. *J. Org. Chem.* **2002**, *67*, 7057.
(37) Hong, B. H. M. S. Thesis, Pohang University of Science and Technology, 1999.
(38) Sinnokrot, M. O.; Sherrill, C. D. *J. Phys. Chem. A* **2003**, *107*, 8377.
(39) Jeziorski, B.; Moszynski, R.; Szalewicz, K. *Chem. Rev.* **1994**, *94*, 1887.
(40) Williams, H. L.; Szalewicz, K.; Jeziorski, B.; Moszynski, R.; Rybak, S. *J. Chem. Phys.* **1993**, *98*, 1279.
(41) Kendall, R. A.; Dunning, T. H.; Harrison, R. J. *J. Chem. Phys.* **1992**, *96*, 6796.

distance between the centers of the rings while keeping the monomers rigid. Changes in the relative orientation between the two aromatic rings was not considered in this initial study. For the benzene dimer, rotation of one ring about the axis joining the centers of mass of the two rings has very little effect on the energy.[17] For the present substituted benzenes, changes in the relative orientation of the two rings will lead to larger energy differences, depending on the substituent. For example, preliminary data suggest that rotating the upper benzene in **4** so that the upper benzene is coplanar with the C−X bond of the substituent leads to direct interactions between the substituent and the meta hydrogen of the upper benzene which are worth a few tenths of one kcal mol^{-1}. We hope to explore these additional complications in future work.

MP2 interaction energies using the larger, aug-cc-pVTZ basis set were approximately corrected for higher-order electron correlation effects by adding the difference between the CCSD(T) and MP2 energies as computed using a modified aug-cc-pVDZ basis, denoted aug-cc-pVDZ′, which lacks diffuse functions on hydrogen and diffuse *d* functions on carbon. This provides an estimate of the CCSD(T)/aug-cc-pVTZ binding energies and interfragment distances. The counterpoise (CP) correction of Boys and Bernardi[42] was applied in all calculations to account for basis set superposition error because our previous work demonstrates that CP-corrected MP2 energies converge more quickly to the complete basis set limit for π-π interactions.[17] Core orbitals were constrained to remain doubly occupied in all correlated wave functions. All supermolecular results in the present study were obtained using the PSI 3.2[43] and MOLPRO[44] programs.

SAPT Approach. Symmetry-adapted perturbation theory (SAPT)[39,40] was employed to analyze the interaction energy in terms of physically meaningful components such as electrostatic, induction, dispersion, and exchange energies. Here, we will employ the original notation of Jeziorski and co-workers.[45] In SAPT, the Hamiltonian of the dimer is decomposed into three parts as $H = F + W + V$, where F is the Fock operator, representing the sum of the Fock operators for the separate monomers; W is the intramonomer correlation operator, accounting for the intramonomer correlation effects; and V is the intermolecular interaction operator. The SAPT interaction energy can be represented as

$$E_{\mathrm{int}} = E_{\mathrm{int}}^{\mathrm{HF}} + E_{\mathrm{int}}^{\mathrm{CORR}}$$

where E_{int}^{HF} represents lowest-order corrections that be can identified as describing interactions at the Hartree−Fock level. $E_{\mathrm{int}}^{\mathrm{HF}}$ can be represented as

$$E_{\mathrm{int}}^{\mathrm{HF}} = E_{\mathrm{elst}}^{(10)} + E_{\mathrm{exch}}^{(10)} + E_{\mathrm{ind,resp}}^{(20)} + E_{\mathrm{exch-ind,resp}}^{(20)} + \delta E_{\mathrm{int,resp}}^{\mathrm{HF}}$$

The superscripts (ab) denote orders in perturbation theory with respect to operators V and W, respectively. It can be seen from the above equation that the HF interaction energy includes first-order polarization and exchange, and second-order induction and exchange-induction contributions. The subscripts "resp" indicate that the induction and exchange-induction contributions include the coupled-perturbed HF response.[40] $\delta E_{\mathrm{int}}^{\mathrm{HF}}$contains the third- and higher-order HF induction and exchange induction contributions.

We have employed the SAPT2 approach, in which the correlated portion of the interaction energy is nearly equivalent to the supermolecular MP2 correlation energy and can be represented as

$$E_{\mathrm{int}}^{\mathrm{CORR}} = E_{\mathrm{elst,resp}}^{(12)} + E_{\mathrm{exch}}^{(11)} + E_{\mathrm{exch}}^{(12)} + {}^{t}E_{\mathrm{ind}}^{(22)} + {}^{t}E_{\mathrm{exch-ind}}^{(22)} + E_{\mathrm{disp}}^{(20)} + E_{\mathrm{exch-disp}}^{(20)}$$

where ${}^{t}E_{\mathrm{ind}}^{(22)}$ represents the part of $E_{\mathrm{ind}}^{(22)}$ that is not included in $E_{\mathrm{ind,resp}}^{(20)}$, and ${}^{t}E_{\mathrm{exch-ind}}^{(22)}$ is approximated as

$${}^{t}E_{\mathrm{exch-ind}}^{(22)} \approx E_{\mathrm{exch-ind,resp}}^{(20)} \frac{{}^{t}E_{\mathrm{ind}}^{(22)}}{E_{\mathrm{ind,resp}}^{(20)}}$$

All SAPT calculations reported here have been carried out using the above-mentioned aug-cc-pVDZ′ basis set with the MP2/aug-cc-pVTZ optimized monomer geometries. For the dimers considered in this study, the aug-cc-pVDZ′ basis set ranges in size from 276 to 307 basis functions; the very high computational cost of the SAPT procedure precludes the use of a larger basis set. SAPT computations were performed using the SAPT2002 program.[45]

Table 1. Interaction Energies (in kcal mol^{-1}) for Various Dimers[a]

		sandwich		T-shaped		T-shaped(2)	
X	method	R^b	ΔE_{int}	R^b	ΔE_{int}	R^b	ΔE_{int}
H	MP2/aug-cc-pVDZ[c]	3.80	−2.90	5.01	−3.16	5.01	−3.16
	MP2/aug-cc-pVTZ[c]	3.70	−3.26	4.89	−3.46	4.89	−3.46
	MP2/aug-cc-pVQZ[d]		−3.37		−3.54		−3.54
	MP2−R12/A[d]		−3.64		−3.63		−3.63
	ΔCCSD(T)/aug-cc-pVDZ′[e,f]		1.26		0.76		0.76
	estd. CCSD(T)/aug-cc-pVTZ[f]	3.90	**−1.80**	4.99	**−2.62**	4.99	**−2.62**
	ΔCCSD(T)/aug-cc-pVDZ[d]		1.83		0.89		0.89
	estd. CCSD(T)/CBS[d]		−1.81		−2.74		−2.74
OH	MP2/aug-cc-pVDZ[c]	3.70	−3.40	5.00	−3.14	4.95	−3.23
	MP2/aug-cc-pVTZ[c]	3.60	−3.75	4.90	−3.42	4.90	−3.52
	ΔCCSD(T)/aug-cc-pVDZ′[f]		1.44		0.77		0.75
	estd. CCSD(T)/aug-cc-pVTZ[f]	3.80	**−2.17**	5.00	**−2.58**	5.00	**−2.67**
CH_3	MP2/aug-cc-pVDZ[c]	3.70	−3.58	5.00	−3.11	4.90	−3.60
	MP2/aug-cc-pVTZ[c]	3.65	−3.96	4.90	−3.39	4.80	−3.89
	ΔCCSD(T)/aug-cc-pVDZ′[f]		1.55		0.78		0.81
	estd. CCSD(T)/aug-cc-pVTZ[f]	3.80	**−2.27**	5.00	**−2.55**	5.00	**−2.95**
F	MP2/aug-cc-pVDZ[c]	3.70	−3.50	4.95	−3.35	5.00	−2.87
	MP2/aug-cc-pVTZ[c]	3.70	−3.81	4.90	−3.61	4.90	−3.17
	ΔCCSD(T)/aug-cc-pVDZ′[f]		1.40		0.74		0.73
	estd. CCSD(T)/aug-cc-pVTZ[f]	3.80	**−2.29**	5.00	**−2.77**	5.00	**−2.38**
CN	MP2/aug-cc-pVDZ[c]	3.70	−4.49	4.90	−3.79	5.00	−2.82
	MP2/aug-cc-pVTZ[c]	3.60	−4.86	4.80	−4.11	4.90	−3.08
	ΔCCSD(T)/aug-cc-pVDZ′[f]		1.58		0.84		0.81
	estd. CCSD(T)/aug-cc-pVTZ[f]	3.80	**−3.05**	4.90	**−3.25**	5.00	**−2.20**

[a] All computations reflect counterpoise correction. [b] Distance from center of benzene ring to center of aromatic ring containing the substituent. [c] Optimized geometry (monomer kept rigid) at each level of theory. [d] Using the best estimates of monomer geometry (C−C = 1.3915, C−H = 1.0800 Å) from ref 17, and intermolecular distance optimized using counterpoise-corrected MP2/aug-cc-pVTZ. [e] aug-cc-pVDZ′ represents a cc-pVDZ basis on hydrogen and an aug-cc-pVDZ basis minus diffuse d functions on other atoms. [f] Using monomer geometry optimized with MP2/aug-cc-pVTZ and intermolecular distance optimized using estimated counterpoise-corrected CCSD(T)/aug-cc-pVTZ.

Results and Discussion

Supermolecular Approach. Theoretical results for binding energies and optimum intermonomer distances are summarized in Table 1. The estimated CCSD(T)/aug-cc-pVTZ results show that all of the substituted sandwich dimers are bound more strongly than benzene dimer, confirming our earlier report on

(42) Boys, S. F.; Bernardi, F. *Mol. Phys.* **1970**, *19*, 553.
(43) Crawford, T. D.; Sherrill, C. D.; Valeev, E. F.; Fermann, J. T.; King, R. A.; Leininger, M. T.; Brown, S. T.; Janssen, C. L.; Seidl, E. T.; Kenny, J. P.; Allen, W. D. *PSI 3.2*, 2003.
(44) Amos, R. D.; Bernhardsson, A.; Berning, A.; Celani, P.; Cooper, D. L.; Deegan, M. J. O.; Dobbyn, A. J.; Eckert, F.; Hampel, C.; Hetzer, G.; Knowles, P. J.; Korona, T.; Lindh, R.; Lloyd, A. W.; McNicholas, S. J.; Manby, F. R.; Meyer, W.; Mura, M. E.; Nicklass, A.; Palmieri, P.; Pitzer, R.; Rauhut, G.; Schütz, M.; Schumann, U.; Stoll, H.; Stone, A. J.; Tarroni, R.; Thorsteinsson, T.; Werner, H.-J. *MOLPRO, a package of ab initio programs designed by Werner, H.-J.; Knowles, P. J. Version 2002.*
(45) Bukowski, R.; Cencek, W.; Jankowski, P.; Jeziorski, B.; Jeziorska, M.; Kucharski, S. A.; Misquitta, A. J.; Moszynski, R.; Patkowski, K.; Rybak, S.; Szalewicz, K.; Williams, H. L.; Wormer, P. E. S. *SAPT2002: An Ab Initio Program for Many-Body Symmetry-Adapted Perturbation Theory Calculations of Intermolecular Interaction Energies. Sequential and Parallel Versions*, 2003.

the sandwiches.[38] Although the OH, CH_3, and F substituents increase binding in the sandwich by 0.4−0.5 kcal mol^{-1} at the best level of theory, CN has a much larger effect of 1.3 kcal mol^{-1}. The substituted T-shaped dimers **3b**−**e** and **4b**−**e**, by contrast, show both increases and decreases in binding relative to benzene dimer, depending on the substituent. Changes in binding due to substitution are smaller for dimers **3** and **4** than for the sandwiches **2**, but once again CN has by far the largest effect. Because substituents have a larger stabilizing effect on the sandwich configurations, the energy difference between the sandwich and T-shaped configurations becomes smaller for the substituted dimers than for benzene dimer. For the cyano substituent, the sandwich **2e** actually becomes 0.9 kcal mol^{-1} more stable than the T-shaped dimer **4e**, demonstrating that the preferred orientation in a π−π interaction can be changed by only a modest degree of substitution.

Concerning convergence of the theoretical predictions, we observe that the optimized distance between monomers, *R*, is relatively insensitive to the improvement of the basis set at the MP2 level (so long as the counterpoise correction is employed), but using the larger basis set makes the binding significantly more favorable (∼0.3−0.4 kcal mol^{-1}) for all dimer configurations. The estimated CCSD(T)/aug-cc-pVTZ optimized intermonomer distances are ∼0.1−0.2 Å larger than the MP2 predictions. This means that the estimated CCSD(T)/aug-cc-pVTZ binding energies will differ from those reported previously[38] for the sandwich configurations, where we used MP2/aug-cc-pVTZ interfragment geometries; using the coupled-cluster geometries makes binding more favorable by about 0.2 kcal mol^{-1}, or around 5−10%. The ΔCCSD(T) corrections are significant for all dimers (see Table 1), and they account for the overestimation of the binding energy by the MP2 method.[12,46] This correction is largest for the sandwich configurations, ranging from 1.4 kcal mol^{-1} for benzene-fluorobenzene dimer to 1.8 kcal mol^{-1} for benzene dimer. For the T-shaped and T-shaped(2) dimer configurations, ΔCCSD(T) is 0.7−0.9 kcal mol^{-1}. The large magnitude of ΔCCSD(T) arises both from the coupling of electron pairs in CCSD (which is neglected in MP2) and from the importance of triple substitutions in CCSD(T). A recent study by Hopkins and Tschumper[47] shows that both of these effects are very important in weakly bound dimers, and furthermore that the effect of connected quadruple substitutions is small but possibly nonnegligible.

Given the sensitivity of the binding energies to the basis set and theoretical method, it might appear that one would require the very highest level of theory to accurately predict changes in binding energies due to substitution. Fortunately, however, Table 2 demonstrates that the binding energies relative to benzene dimer are accurately predicted at any of the levels of theory considered here, with variations of less than 0.1 kcal mol^{-1} in most cases. This suggests that even though the absolute binding energies are very difficult to compute reliably, lower levels of theory should be sufficient to predict relative changes due to substitution in future studies of larger molecules.

Sandwich Dimers. As noted above, Table 1 indicates that *all* of the substituted sandwich dimers bind more strongly than benzene dimer. This is a surprising result if we note that these substituents are typically characterized as ranging from strongly electron donating (OH) to strongly electron withdrawing (CN). Our results appear to be inconsistent with the experimental study of Cozzi, Siegel, and co-workers,[29] which indicated a linear relationship between the interaction energies of substituted phenyl groups and the sum of the Hammett parameters σ_{para} of the substituents. In that work, barriers to rotation $\Delta G^{\ddagger}$ about the aryl-naphthyl bond were determined using NMR for a few substituted 1,8-diarylnaphthalenes in which the two phenyl groups are forced into a nearly face-to-face stacked geometry. During rotation about the aryl-naphthyl bond, the stacked interaction is lost, and the authors therefore assumed that the barriers to rotation are determined by the strength of the π−π interaction in the stacked geometry. We note, however, that even in the transition state to rotation, there is still an interaction between the two phenyl groups (although their orientation is now different) which may also be affected by substituents; therefore, the differences in barrier heights for the different substituents may not be determined solely by the differences in the attraction at the stacked geometry. The present theoretical results, which measure the intrinsic interaction energy directly, do not show a good correlation between interaction energy and Hammett σ parameters.

In earlier work on substituted sandwich dimers,[38] we attempted to analyze substituent effects in terms of the Hunter−Sanders rules, which state that although dispersion is critical to making π−π interactions favorable, it is electrostatics which determine changes in binding due to geometry or substitutent effects. For a face-to-face sandwich configuration, the most important consideration would be the negatively charged π-electron cloud above the ring center. Electron withdrawing substituents should reduce the negative π charge and lead to decreased π−π electrostatic repulsion, and vice versa for electron donating substituents. Such a picture seems consistent with the experimental results of Cozzi et al.,[27,28] but it is not consistent with our theoretical binding energies, if one assumes that the Hammett parameters are indicative of the degree of

Table 2. Interaction Energies Relative to Benzene Dimer[a]

	X=H	OH	CH_3	F	CN
sandwich dimers **2a**−**e**					
MP2/aug-cc-pVDZ′[b,c]	0.00	−0.40	−0.54	−0.51	−1.40
MP2/aug-cc-pVDZ[d]	0.00	−0.50	−0.68	−0.60	−1.59
MP2/aug-cc-pVTZ[c]	0.00	−0.49	−0.70	−0.55	−1.60
Est. CCSD(T)/aug-cc-pVTZ[c]	0.00	−0.37	−0.47	−0.49	−1.25
SAPT2/aug-cc-pVDZ′[e]	0.00	−0.49	−0.61	−0.61	−1.56
T-shaped dimers **3a**−**e**					
MP2/aug-cc-pVDZ′[b,c]	0.00	0.02	0.05	−0.17	−0.58
MP2/aug-cc-pVDZ[d]	0.00	0.02	0.05	−0.19	−0.63
MP2/aug-cc-pVTZ[c]	0.00	0.04	0.07	−0.15	−0.65
Est. CCSD(T)/aug-cc-pVTZ[c]	0.00	0.04	0.07	−0.15	−0.63
SAPT2/aug-cc-pVDZ′[e]	0.00	0.03	0.07	−0.21	−0.71
T-shaped(2) dimers **4a**−**e**					
MP2/aug-cc-pVDZ′[b,c]	0.00	−0.04	−0.38	0.27	0.29
MP2/aug-cc-pVDZ[d]	0.00	−0.07	−0.44	0.29	0.34
MP2/aug-cc-pVTZ[c]	0.00	−0.06	−0.44	0.29	0.39
Est. CCSD(T)/aug-cc-pVTZ[c]	0.00	−0.05	−0.33	0.24	0.42
SAPT2/aug-cc-pVDZ′[e]	0.00	−0.04	−0.44	0.30	0.33

[a] All computations reflect counterpoise correction. [b] aug-cc-pVDZ′ represents a cc-pVDZ basis on hydrogen and an aug-cc-pVDZ basis minus diffuse d functions on other atoms. [c] Intermonomer distance optimized at the given level of theory with rigid MP2/aug-cc-pVTZ monomer geometries. [d] Monomer geometry and intermonomer distance optimized at the MP2/aug-cc-pVDZ level of theory. [e] Using MP2/aug-cc-pVTZ optimized monomer geometry and intermolecular distances of 3.7 Å for **2a**−**e** and 4.9 Å for **3a**−**e** and **4a**−**e**.

(46) Jaffe, R. L.; Smith, G. D. *J. Chem. Phys.* **1996**, *105*, 2780.
(47) Hopkins, B. W.; Tschumper, G. S. *J. Phys. Chem. A* **2004**, *108*, 2941.

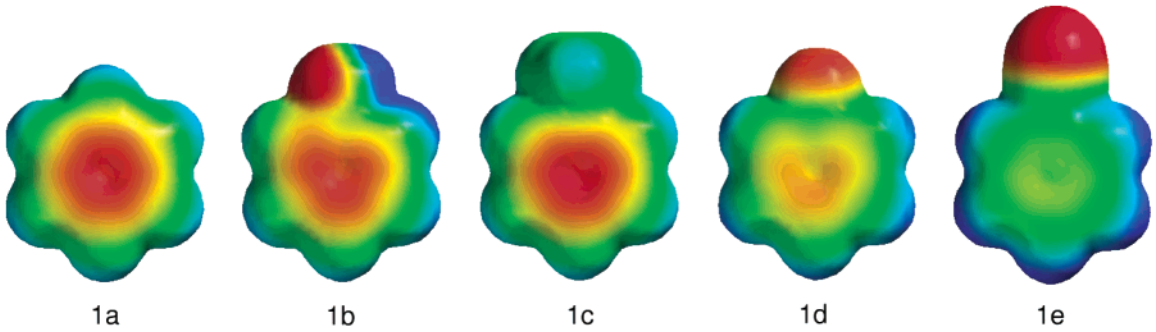

Figure 1. Electrostatic potential computed using Hartree−Fock and 6-31G* basis set with a scale of −25 (red) to 25 kcal mol^{-1} (blue). Potentials using B3LYP/6-31G* appear very similar.

π−electron density. The Hammett σ parameters, however, were determined from the equilibrium constants for the dissociation of substituted benzoic acids,[48] and there is no reason to assume that they necessarily correlate with the π−electron density in the reactants for those dissociations. Indeed, recent work on cation-π interactions by Dougherty and co-workers shows that the hydroxyl group, which is a strongly activating, electron donating substituent in the context of electrophilic aromatic substitution, has nearly the same electrostatic potential above the center of the ring as unsubstituted benzene.[49]

Because the Hunter−Sanders rules propose that electrostatics are the most important consideration, we have computed electrostatic potential maps of the monomers (Figure 1), rather than relying on Hammett σ parameters as an indirect measure of electrostatics. Figure 1 indicates that benzonitrile has the least negative π cloud, followed by fluorobenzene. However, the electrostatic potentials of the π clouds are similar for benzene, toluene, and phenol. Even though OH is electron donating in some other contexts, it has little effect on the electrostatic potential on top of the ring, in agreement with the findings of Dougherty and co-workers.[49]

Unfortunately, even if we ignore the Hammett σ parameters and consider the π charge as it appears from the electrostatic potentials, the Hunter−Sanders rules still do not give us qualitatively correct conclusions. On the basis of the electrostatic potentials in Figure 1, we would expect benzene, toluene, and phenol to have nearly the same binding energies to benzene, which is not the case here (see Table 1). Instead, the difference in binding energies between toluene−benzene and benzene−benzene, which we would expect to be very small, is significantly larger than that between fluorobenzene−benzene and toluene−benzene, which we would expect to be larger. Thus, even though Hunter−Sanders rules are useful in many instances for qualitative predictions of binding energies in π−π interactions, clearly they do not always predict the right trends for substituents because they lack other effects such as dispersion, induction, and exchange-repulsion. Concerning the three monomers (benzene, toluene, phenol) which ought to have similar electrostatic interactions with benzene based on the electrostatic potentials, their binding energies increase in the same order as their polarizabilities,[50] suggesting that dispersion is important in determining the differences between substituted dimers. A more detailed analysis of the binding trends using SAPT is described below.

T-Shaped Dimers. Binding energies for the T-shaped dimers are also summarized in Table 1. Benzene−benzonitrile and benzene−fluorobenzene both bind more strongly than benzene dimer, by 0.63 and 0.15 kcal mol^{-1}, respectively, at the most reliable level of theory. Conversely, benzene−phenol and benzene−toluene are slightly less bound compared to benzene−dimer, by 0.04 and 0.07 kcal mol^{-1}, respectively. These changes are at least partially attributable to the electron donating or electron withdrawing effects of the substituent. Electron withdrawing groups will decrease the exchange-repulsion term and increase the favorable electrostatic interaction between the partial-positive para hydrogen and the negatively charged π-electron cloud of the unsubstituted benzene ring below it; the opposite will happen for electron donating groups. Natural population analysis charges computed for the substituted monomers (B3LYP/cc-pVDZ) indicate relatively small changes ($\leq$ 0.004 au) in the para hydrogen charge except in benzonitrile (0.008 au), and the SAPT analysis below demonstrates that the largest changes generally come in the exchange-repulsion term, not the electrostatic term.

T-Shaped(2) Dimers. As shown in Chart 1, in the T-shaped-(2) dimers, a hydrogen from benzene points downward at the center of the ring of the substituted monomer. In this case, we expect changes in binding energies to correlate with the π-donating or withdrawing capacity of the substituents. A π-donating substituent should increase the negative charge of the π cloud on the substituted benzene, leading to a more favorable electrostatic interaction with the partial positive charge on the hydrogen pointing down at it. The electrostatic potential maps plotted in Figure 1 suggest that binding should be similar for benzene, phenol, and toluene, smaller for fluorobenzene, and smallest for benzonitrile. Indeed, the decreases in binding energies compared to benzene dimer for benzene-fluorobenzene and benzene−benzonitrile are 0.24 kcal mol^{-1} and 0.42 kcal mol^{-1}, respectively, compared to benzene dimer. The binding energy of benzene−phenol is very similar to that of benzene dimer (0.05 kcal mol^{-1} more stable), as expected. However, the binding energy of toluene is significantly increased, by 0.33 kcal mol^{-1}. Our SAPT analysis (below) indicates that this is due to a greater dispersion energy for benzene-toluene than for benzene-phenol or benzene dimer.

According to the preceding analysis of supermolecular binding energies, it is clear that consideration of electrostatic

(48) Hammett, L. P. *J. Am. Chem. Soc.* **1937**, *59*, 96.
(49) Mecozzi, S.; West, A. P.; Dougherty, D. A. *Proc. Natl. Acad. Sci. U.S.A.* **1996**, *93*, 10 566.
(50) Maryott, A. A.; Buckley, F., *U.S. National Bureau of Standards Circular No. 537*, 1953.

Table 3. Contributions to the Interaction Energy (kcal mol^{-1}) for Different Sandwich Dimer Configurations **2a**−**e**[a]

	X=H	OH	CH_3	F	CN
E_{int}^{HF}	5.330	4.947	5.352	4.534	3.914
$E_{elst}^{(10)}$	−0.520	−0.689	−0.544	−1.073	−1.757
$E_{exch}^{(10)}$	6.185	5.984	6.299	5.900	5.968
$E_{ind,r}^{(20)}$	−2.196	−2.252	−2.291	−2.153	−2.150
$E_{exch-ind,r}^{(20)}$	2.002	2.058	2.066	2.010	2.005
$\delta E_{int,r}^{HF}$	−0.141	−0.153	−0.179	−0.150	−0.151
$E_{elst,r}^{(12)}$	−0.454	−0.388	−0.483	−0.282	−0.075
$E_{exch}^{(11)} + E_{exch}^{(12)}$	−0.151	−0.132	−0.089	−0.169	−0.190
$^tE_{ind}^{(22)}$	0.054	0.035	0.043	0.038	0.049
$^tE_{exch-ind}^{(22)}$	−0.050	−0.032	−0.039	−0.036	−0.046
$E_{disp}^{(20)}$	−7.470	−7.653	−8.173	−7.377	−7.909
$E_{exch-disp}^{(20)}$	0.942	0.933	0.985	0.888	0.899
$E_{int}(SAPT2)$	**−1.798**	**−2.289**	**−2.405**	**−2.403**	**−3.357**
$E_{int}(MP2)$[b]	−1.744	−2.223	−2.345	−2.326	−3.273

[a] Using MP2/aug-cc-pVTZ optimized monomer geometry and intermolecular distance of 3.7 angstroms. [b] MP2/aug-cc-pVDZ′ counterpoise-corrected binding energies.

effects alone (as advanced by the Hunter-Sanders rules) is not sufficient to fully explain the trends in the binding energies of the substituted dimers. To better understand the observed trends, we now turn to SAPT to decompose the binding energy into its electrostatic, dispersion, induction, and exchange-repulsion components.

SAPT Approach. All SAPT computations were performed using MP2/aug-cc-pVTZ optimized monomer geometries. The individual energy components of the SAPT analysis were found to be very sensitive to the interfragment distance; for example, when T-shaped benzene-benzonitrile **3e** is computed at distances of 4.8 and 4.9 Å, the exchange-repulsion term changes by 35%, and the $E_{disp}^{(20)}$ dispersion term changes by 16%. Such changes were often larger than the variations due to substituent effects. For that reason, we performed all SAPT computations at the same intermonomer distances: 3.7 Å for the sandwiches **2**, and 4.9 Å for the T-shaped configurations **3** and **4**. All SAPT computations were carried out using the modified aug-cc-pVDZ′ basis. Critical to our SAPT analysis is the ability of such a modest basis set to faithfully reproduce the higher-level supermolecular (SM) ordering of the binding energies for the dimers studied. Table 2 indicates that the shifts in binding energies due to substituents are reliably predicted by SAPT2/aug-cc-pVDZ′ (despite our using the same interfragment distance for all dimers of a given configuration, which is not the equilibrium distance in all cases).

Sandwich Dimers. The SAPT binding energies for the sandwich dimers are summarized in Table 3. The electrostatic component of the binding energy, represented here by the sum of $E_{elst}^{(10)}$ and $E_{elst,r}^{(12)}$, is always stabilizing. This is surprising from the point of view of the Hunter-Sanders model, which would imagine two negatively charged π clouds directly on top of each other for the benzene dimer sandwich. However, such a picture ignores the fact that the electron clouds interpenetrate, and the electrostatic penetration term is usually attractive. The electrostatic energies for the T-shaped dimers **3** and **4** (Tables 4 and 5) are much more attractive than for the sandwiches **2**, in agreement with the expected dominance of attractive $\sigma-\pi$ interactions in the T-shaped configuration. The exchange-repulsion terms are substantially larger than the attractive

Table 4. Contributions to the Interaction Energy (kcal mol^{-1}) for Different T-Shaped Dimer Configurations **3a**−**e**[a]

	X=H	OH	CH_3	F	CN
E_{int}^{HF}	1.618	1.677	1.817	1.228	0.648
$E_{elst}^{(10)}$	−2.190	−2.135	−2.131	−2.293	−2.770
$E_{exch}^{(10)}$	4.447	4.442	4.588	4.171	4.219
$E_{ind,r}^{(20)}$	−1.161	−1.152	−1.189	−1.105	−1.210
$E_{exch-ind,r}^{(20)}$	0.914	0.907	0.946	0.836	0.847
$\delta E_{int,r}^{HF}$	−0.392	−0.385	−0.397	−0.382	−0.438
$E_{elst,r}^{(12)}$	−0.054	−0.071	−0.104	0.022	0.181
$E_{exch}^{(11)} + E_{exch}^{(12)}$	0.418	0.405	0.431	0.376	0.374
$^tE_{ind}^{(22)}$	−0.144	−0.139	−0.154	−0.117	−0.105
$^tE_{exch-ind}^{(22)}$	0.113	0.109	0.123	0.089	0.073
$E_{disp}^{(20)}$	−4.893	−4.896	−5.004	−4.713	−4.772
$E_{exch-disp}^{(20)}$	0.526	0.529	0.547	0.489	0.478
$E_{int}(SAPT2)$	**−2.415**	**−2.385**	**−2.344**	**−2.626**	**−3.122**
$E_{int}(MP2)$[b]	−2.248	−2.241	−2.189	−2.464	−2.888

[a] Using MP2/aug-cc-pVTZ optimized monomer geometry and intermolecular distance of 4.9 angstroms. [b] MP2/aug-cc-pVDZ′ counterpoise-corrected binding energies.

Table 5. Contributions to the Interaction Energy (kcal mol^{-1}) for Different T-Shaped(2) Dimer Configurations **4a**−**e**[a]

	X=H	OH	CH_3	F	CN
E_{int}^{HF}	1.618	1.674	1.365	1.971	2.295
$E_{elst}^{(10)}$	−2.190	−2.065	−2.343	−1.816	−1.510
$E_{exch}^{(10)}$	4.447	4.365	4.374	4.333	4.293
$E_{ind,r}^{(20)}$	−1.161	−1.167	−1.179	−1.118	−1.110
$E_{exch-ind,r}^{(20)}$	0.914	0.930	0.914	0.929	0.939
$\delta E_{int,r}^{HF}$	−0.392	−0.389	−0.401	−0.355	−0.316
$E_{elst,r}^{(12)}$	−0.054	−0.119	−0.036	−0.161	−0.218
$E_{exch}^{(11)} + E_{exch}^{(12)}$	0.418	0.417	0.435	0.400	0.393
$^tE_{ind}^{(22)}$	−0.144	−0.158	−0.146	−0.158	−0.154
$^tE_{exch-ind}^{(22)}$	0.113	0.126	0.113	0.131	0.130
$E_{disp}^{(20)}$	−4.893	−4.932	−5.120	−4.802	−5.032
$E_{exch-disp}^{(20)}$	0.526	0.519	0.534	0.500	0.498
$E_{int}(SAPT2)$	**−2.415**	**−2.474**	**−2.854**	**−2.117**	**−2.087**
$E_{int}(MP2)$[b]	−2.248	−2.316	−2.687	−1.967	−1.963

[a] Using MP2/aug-cc-pVTZ optimized monomer geometry and intermolecular distance of 4.9 angstroms. [b] MP2/aug-cc-pVDZ′ counterpoise-corrected binding energies.

electrostatic terms in the sandwiches, so that the sum of the electrostatic and exchange terms is overall repulsive.

Because CN is the most strongly electron withdrawing substituent, it should reduce the π density the most, decreasing unfavorable $\pi-\pi$ repulsion. Indeed, we observe the most favorable electrostatic energy for benzene-benzonitrile (0.86 kcal mol^{-1} more stable than benzene dimer). The next most favorable electrostatic energy is for benzene-fluorobenzene, which is consistent with F being the next most effective electron withdrawing substituent, as indicated by the electrostatic potentials in Figure 1. According to that figure, the electrostatic energies should be nearly the same for the sandwiches of benzene with benzene, phenol, and toluene, and this is what we observe in Table 3. Hence, the trends in electrostatic energies with respect to substitution seem consistent with expectations based on electrostatic potential maps of the monomers. Because the electrostatic energies for benzene−phenol and benzene−toluene are so similar to that of benzene dimer, clearly electrostatics alone cannot explain why the *total* binding energies of those dimers are significantly larger than that of benzene

dimer. Other energetic components are therefore important in determining the energetic order of the dimers.

The exchange energy terms calculated here are $E_{exch}^{(10)}$, $E_{exch-ind,r}^{(20)}$, $E_{exch}^{(11)}$, $E_{exch}^{(12)}$, ${}^tE_{exch-ind}^{(22)}$, and $E_{exch-disp}^{(20)}$. $E_{exch}^{(10)}$ accounts for the repulsion due to the Pauli exclusion principle and arises from the antisymmetry requirement of the wave function, $E_{exch}^{(11)}$ and $E_{exch}^{(12)}$ account for the effects of intramonomer correlation on the exchange repulsion, and $E_{exch-ind,r}^{(20)}$ and other second-order terms (${}^tE_{exch-ind}^{(22)}$ and $E_{exch-disp}^{(20)}$) account for additional exchange repulsion arising from the coupling of electron exchange and the induction and dispersion interactions. The exchange energy is slightly more repulsive for benzene−toluene and slightly less repulsive for benzene−phenol, benzene−fluorobenzene, and benzene−benzonitrile, than in benzene dimer. This is consistent with the reduced $\pi-\pi$ overlap for the electron withdrawing CN and F substituents and the increased $\pi-\pi$ overlap for the weakly electron donating CH_3 group. Kim and co-workers previously noted a similar reduction in exchange-repulsion energies for fluorobenzene−argon as compared to benzene−argon.[51] The relative exchange energies are larger in magnitude than the relative electrostatic energies for CH_3 and OH substituents, indicating the importance of exchange terms. When the exchange-induction and exchange-dispersion cross terms are counted as induction and dispersion, respectively, the relative exchange energy for the OH substituent (compared to benzene dimer) is almost twice as large as the relative electrostatic energy.

The induction contribution to the binding energy is mainly contained in $E_{ind,r}^{(20)}$. This is a second-order energy correction that results from the distortion of the charge distribution of one monomer by the electrostatic charge distribution of other monomer, and vice versa. This mutual polarization of the monomer by the static electric field of the other is proportional to the multipole moments and static polarizabilities of the monomers. The leading intramonomer correlation contribution is included in ${}^tE_{ind}^{(22)}$ and accounts for only 2% of the induction energy. Table 3 shows that the dominant induction term $E_{ind,r}^{(20)}$ is very similar for all sandwich dimers. The attractive part of the induction energy is substantially quenched by the repulsive exchange-induction energy (represented by $E_{exch-ind,r}^{(20)}$ and ${}^tE_{exch-ind}^{(22)}$). As noted by Jeziorski and co-workers,[39] any quantitatively accurate calculation of the induction energy cannot neglect the exchange-induction contribution. If we account for this repulsive term and also add the third- and higher-order induction and exchange-induction terms in δE_{int}^{HF}, induction stabilizes the total binding energy by 0.3−0.4 kcal mol^{-1} for the sandwich dimers investigated. The shifts in the induction energies relative to benzene dimer due to substitution are less than 0.07 kcal mol^{-1}.

Dispersion stabilizes the binding energy of the sandwich dimers by 6.5 to 7.2 kcal mol^{-1} after the exchange-dispersion correction. This is by far the largest attractive contribution. Figure 2 displays the good correlation between dispersion energies and the π components of the polarizabilities of the substituted monomers, computed at the HF/aug-cc-pVDZ level (46.2 **1a**, 47.4 **1b**, 54.9 **1c**, 44.7 **1d**, and 51.8 $e^2a_o^2/E_h$ **1e**). The dispersion energies relative to benzene dimer **2a** are significant for all but the F substituent, ranging from −0.66 to 0.04 kcal mol^{-1}. For methyl-substituted **2c**, dispersion is the most important contributor to the energy lowering relative to benzene dimer **2a**. For hydroxyl-substituted **2b**, dispersion is twice as important as electrostatics in contributing to the stabilization relative to **2a**.

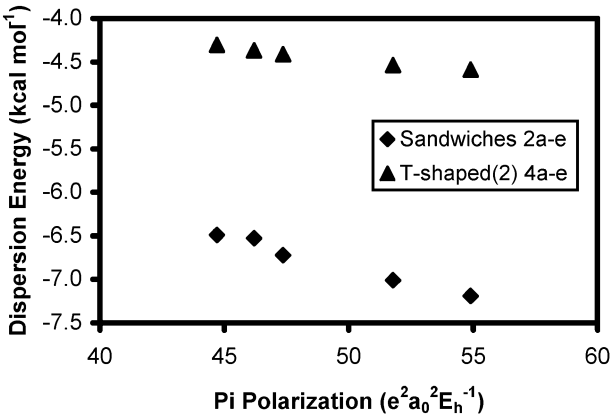

Figure 2. Plot of dispersion energy (SAPT2/aug-cc-pVDZ′, exchange-corrected) vs polarizability in the direction perpendicular to the aromatic plane (HF/aug-cc-pVDZ).

T-Shaped Dimers. Table 4 shows the SAPT contributions to the interaction energy for the T-shaped dimers **3a**−**e**. It should be noted that, in general, the T-shaped dimers have a larger electrostatic component than their sandwich counterparts because of favorable quadrupole-quadrupole interactions. They also exhibit smaller destabilizing exchange-repulsion energies and smaller stabilizing dispersion energies than the sandwich dimers. Nevertheless, the dispersion and exchange-repulsion energies remain larger than the electrostatic energies for **3a**−**e**.

Examining Table 4, we see that the sum of electrostatic terms ($E_{elst}^{(10)} + E_{elst,r}^{(12)}$) is very similar for all of the T-shaped dimers, with differences of 0.04 kcal mol^{-1} or less from benzene dimer except for benzene−benzonitrile. The trend in electrostatic energies follows the trend in computed para hydrogen charges, with the exception of the hydroxyl substituent. The trend in electrostatic energies also happens to match the trend in total binding energies, except for a reversal of the order for the CH_3 and OH substituents. However, due to the very small changes in electrostatic energies due to substitution, and the much larger changes in other energy components (below), this appears fortuitous.

The exchange interactions for the T-shaped dimers are considerably less repulsive than for the sandwiches; this is due to the reduced overlap between the orbitals of the two monomers. Benzene−fluorobenzene and benzene−benzonitrile have smaller (0.32 and 0.27 kcal mol^{-1}, respectively) exchange-repulsion energies than benzene dimer because the F and CN substituents are electron withdrawing and reduce the electron density available to interact with the other benzene. Such a reduction of electron density in the ring also reduces the favorable dispersion contribution by ∼0.1 kcal mol^{-1}. An opposite effect is seen for benzene-toluene because methyl is a slightly electron donating substituent. The increased electron density in the toluene ring leads to a slightly larger exchange repulsion (∼0.2 kcal mol^{-1}) and more favorable dispersion energy (0.1 kcal mol^{-1}) than in benzene dimer. Although

(51) Tarakeshwar, P.; Kim, K. S.; Kraka, E.; Cremer, D. *J. Chem. Phys.* **2001**, *115*, 6018.

substituent effects for exchange and dispersion are of opposite sign, the shifts in the exchange energies are usually 2−4 times larger. Therefore, dispersion is less important in determining relative energies for the T-shaped dimers than for the sandwich dimers. Substitution by OH leads to very small changes in exchange and dispersion energies relative to benzene dimer. Shifts in exchange-corrected induction energies relative to benzene dimer are relatively small and generally have the same sign as the electrostatic shifts. The largest effect due to induction is an 0.2 kcal mol^{-1} increase in binding for the CN substituent.

T-Shaped(2) Dimers. Table 5 shows the SAPT contributions to the interaction energy for substituted T-shaped(2) dimers **4a**−**e**. Now the substituent will either enhance or reduce the π-electron density on the lower benzene ring, and consequently, increase or decrease its electrostatic interaction with the partial positive charge of the hydrogen on the upper benzene. The electron withdrawing F and CN substituents reduce the amount of π-electron density on the lower ring and decrease both the electrostatic interaction (by 0.27 and 0.52 kcal mol^{-1}, respectively) and the total binding energy (by 0.30 and 0.33 kcal mol^{-1} at the SAPT2 level). The electron donating methyl substituent has the opposite effect, increasing the electrostatic attraction by 0.14 kcal mol^{-1} and the total binding energy by 0.44 kcal mol^{-1}. Once again the OH substituent has little effect, with a decrease in electrostatic attraction of 0.06 kcal mol^{-1} and an increase in total binding of the same size. Other than this sign change for OH, the trend in total binding energies follows that of the electrostatic interaction. We observe once again that the exchange-corrected induction energies are relatively small, and their shifts relative to benzene dimer have the same sign but are several times smaller than the shifts in the electrostatic energies.

Although the relative energies generally follow the same trend as the electrostatic energies, that does not mean that the electrostatic contribution to the total energy is the dominant one. As was seen for **3**, both the exchange and dispersion energies are greater in magnitude than the electrostatic energies for **4**. This agrees with Wilcox's conclusion,[32] based on the molecular torsion balance, that "the electrostatic potential of the aromatic ring is *not* a dominant aspect of the aryl−aryl interaction."

We might expect that the F and CN substituents, by reducing the amount of π-electron density directly below the hydrogen from the other benzene, should also decrease the exchange repulsion relative to benzene dimer. This expectation is fulfilled by reductions of 0.13 and 0.18 kcal mol^{-1} in the exchange energies for F and CN, respectively. On the other hand, the exchange energy for the CH_3 substituent is also decreased (by 0.06 kcal mol^{-1}), in contrast to its modest electron donating character.

As for the sandwich configuration, we observe a correlation between dispersion energies and the computed π polarizability of the monomers (see Figure 2). The relative dispersion energy is comparable to the relative electrostatic energy for hydroxyl-substituted **4b**, and it is larger than the relative electrostatic energy for methyl-substituted **4c**. Hence, the electrostatic energy largely determines the energetic order of the T-shaped dimers **4**, but other effects remain important in determining the size of the relative energies.

Conclusions

A better understanding of π−π interactions will aid rational design efforts in biological chemistry and crystal engineering. Substituent effects in the sandwich and T-shaped configurations of benzene dimer have been quantified using an additive scheme to estimate high-quality theoretical CCSD(T)/aug-cc-pVTZ binding energies and interfragment distances. The cyano substituent has by far the largest effect, changing the binding energy by more than 1 kcal mol^{-1} relative to benzene dimer in some cases; this substituent is even capable of making the sandwich configuration drop lower in energy than one of the T-shaped configurations. In general, fluorine has the next largest effect, followed by methyl and then hydroxyl. Unlike previous experimental studies, the present work does not show a good correlation between binding energies and Hammett parameters (although a rough correlation with σ_{meta} is seen for the T-shaped dimers).

To uncover the origin of the observed trends in binding energies, we performed the first symmetry-adapted perturbation theory (SAPT2) decomposition of π−π interaction energies into their electrostatic, dispersion, induction, and exchange-repulsion components. Dispersion and exchange-repulsion are more important than electrostatics in determining the total binding energies of the dimers considered. Induction energies are largely quenched by exchange-induction coupling, and they contribute very little to differences in binding energies between the substituted dimers. Contrary to the predictions of the Hunter-Sanders rules, electrostatics alone are insufficient to predict the correct trends in binding. For the sandwich configuration, electrostatics suggest that phenol and toluene should bind to benzene about as well as benzene does; however, both of them actually bind more strongly by 0.4−0.5 kcal mol^{-1}. For several T-shaped dimers, either exchange or dispersion makes larger contributions to the relative energy than electrostatics. This suggests that models based solely on electrostatic effects will have difficulty in reliably predicting substituent effects in π−π interactions.

Acknowledgment. We thank Prof. Daniel Crawford (Virginia Tech) for providing the code to evaluate polarizabilities. C.D.S. is a Blanchard Assistant Professor of Chemistry at Georgia Tech and acknowledges a Camille and Henry Dreyfus New Faculty Award and an NSF CAREER award (Grant No. CHE-0094088). The Center for Computational Molecular Science and Technology is funded through a Shared University Research (SUR) grant from IBM and by Georgia Tech. We gratefully acknowledge partial support by the Molecular Design Institute at Georgia Tech, under Prime contract N00014-95-1-1116 from the Office of Naval Research.

Supporting Information Available: A .txt file of Cartesian coordinates of dimers. This material is available free of charge via the Internet at http://pubs.acs.org.

JA049434A